

**Nitrogen dioxide and kerosene-flame soot calibration of photoacoustic instruments for  
measurement of light absorption by aerosols**

W. Patrick Arnott, Hans Moosmüller, and John W. Walker  
Desert Research Institute  
Reno NV 89512

**ABSTRACT**

A nitrogen dioxide calibration method is developed to evaluate the theoretical calibration for a photoacoustic instrument used to measure light absorption by atmospheric aerosols at a laser wavelength of 532.0 nm. This method uses high concentrations of nitrogen dioxide so that both a simple extinction and the photoacoustically-obtained absorption measurement may be performed simultaneously. Since Rayleigh scattering is much less than absorption for the gas, the agreement between the extinction and absorption coefficients can be used to evaluate the theoretical calibration, so that the laser gas spectra are not needed. Photoacoustic theory is developed to account for strong absorption of the laser beam power in passage through the resonator. Findings are that the photoacoustic absorption based on heat-balance theory for the instrument compares well with absorption inferred from the extinction measurement, and that both are well-within values represented by published spectra of nitrogen dioxide. Photodissociation of nitrogen dioxide limits the calibration method to wavelengths longer than 398 nm. Extinction and absorption at 532 nm and 1047 nm was measured for kerosene-flame soot to evaluate the calibration method, and the single scattering albedo was found to be 0.31 and 0.20 at these wavelengths, respectively.

## 1. Introduction

Aerosol optical properties, including light absorption, scattering, extinction, and phase function, are needed to quantify and understand visibility at scenic areas,<sup>1</sup> and, more generally, atmospheric radiation transfer. Aerosol light absorption at visible wavelengths is predominately due to the so-called black carbon aerosol (soot), and the primary source of this aerosol is combustion.<sup>2</sup> Filter-based methods are commonly used to infer aerosol light absorption through the attenuation of light across the aerosol-laden filter. These methods are generally adequately precise and simple in practice, though calibration and operation require aerosol extinction and scattering measurements in the laboratory, and use of a nephelometer to obtain the aerosol scattering correction in the field.<sup>3</sup> In addition, these methods may be susceptible to artifact when the relative humidity increases sufficiently high that aerosols deliquesce, and aqueous solution forms on the filter substrate. Aerosol light absorption can also be measured with a photoacoustic instrument to calibrate and complement filter-based methods.<sup>4-7</sup>

The absorption coefficient is the primary quantity measured with a photoacoustic instrument.<sup>5</sup> A basic description of the method is as follows. A continuous sample of aerosol-laden air is drawn through an acoustic resonator equipped with a microphone and with windows to allow passage of a laser beam through the resonator (Fig. 1). The laser beam (or more generally, the light source) is power-modulated at a frequency that matches the resonance acoustic frequency of the resonator. Light absorption by aerosols causes periodic heating of the gas in the resonator. The heated gas expands, creating a sound source. The microphone signal is a measure of the heat generated by light absorption. By use of a calibrated microphone, a calibrated photodetector to measure laser power, a calibrated acoustic resonator, and simple linear theory for the sound at the microphone by the laser-beam light-absorption source, one

obtains the absorption coefficient. Light absorption can be directly measured for aerosols in-situ, and no filters are needed.

Laser-based photoacoustic instruments are also routinely used in trace-gas spectroscopy,<sup>8-</sup><sup>10</sup> and have been used to monitor black carbon content of vehicle exhaust.<sup>11</sup> A common method for calibration is to place a known concentration of light absorbing gas in the resonator and to measure the resultant microphone signal.<sup>12</sup> This method is limited by the accuracy of the gas concentration determination, the accuracy and resolution of both gas and laser spectra. A common method of calibrating for black carbon content is to use the slope of a linear regression of microphone signal versus elemental carbon content obtained via thermal methods.<sup>13</sup> While this method appears to be adequate for black carbon content determination, the next step of producing a light absorption coefficient for aerosol optics applications is left unfinished.

The calibration method developed in this paper uses sufficiently high concentrations of absorbing gas in the resonator to obtain both the extinction (from gas transmissivity) and absorption (photoacoustic measurement). Extinction is sufficiently large that Rayleigh scattering can be ignored when seeking closure between extinction and absorption. Theory is developed to accommodate the loss of laser power in the resonator due to strong extinction. It is found that the theory for obtaining light absorption in a calibrated resonator (known quality factor and resonance frequency) along with use of a calibrated microphone (known acoustic pressure for a given microphone voltage) and calibrated photodetector (known laser power for a given photodetector voltage) produces a light absorption coefficient that agrees well with the measured extinction coefficient, and with the independently-measured high resolution spectrum and concentration of NO<sub>2</sub>.

## 2. Photoacoustic theory for calibration by strongly absorbing gas in the resonator.

While a thorough description of the plane wave photoacoustic instrument has been given,<sup>5</sup> the basic elements for the present discussion are given in Fig. 1. The acoustic resonator is a full-wavelength resonator with pressure antinodes at the ends and center, and 45 deg. bends near the pressure nodes to accommodate laser beam insertion. A laser beam, with power modulated at the acoustic resonance frequency (e.g., with a mechanical chopper), enters and exits the resonator through holes in the resonator wall placed at pressure nodes. The holes are much smaller in diameter than the acoustic wavelength, and, being at the pressure nodes, negligibly influence resonator acoustics. This arrangement also helps reduce the coupling of noise into the resonator at the acoustic frequency. The laser beam power amplitude and phase (e.g. relative to the chopper sync) at the modulation frequency are obtained from a fast photodetector and phase sensitive detection. Sound is generated by light absorption near the center of the resonator, in the region of a pressure antinode. A capacitive microphone, with its membrane acting as the resonator wall at the left end, is used to measure the amplitude and phase of the sound produced at the acoustic frequency. A thin piezoelectric disk forms the right termination of the resonator, and it is used as an acoustic driver, alternating with the light absorption measurement, in a rapid swept sinusoidal scan to obtain resonator acoustic calibration (resonance frequency and quality factor). The method for doing the acoustic calibration has been previously described.<sup>14</sup>

Theoretical analysis of the instrument in Fig. 1 provides the absorption coefficient,  $B_{abs}^{(0)}$ , from measured quantities,

$$B_{abs}^{(0)} = \frac{P_{mic}(f_r)}{P_L(f_r)} \frac{\pi^2 f_r A_{res}}{Q(\gamma - 1)} \quad , \quad (1)$$

where  $P_{mic}(f_r)$  and  $P_L(f_r)$  are the amplitude of the microphone pressure and laser power at the acoustic resonance frequency  $f_r$ ,  $A_{res}$  is the cross sectional area of the resonator,  $Q$  is the resonator quality factor, and  $\gamma$  is the ratio of the isobaric to isochoric specific heats for the gas in the resonator.<sup>5</sup> The superscript (0) is a reminder that this equation is valid for  $B_{abs}^{(0)}D \ll 1$ , where, referring to Fig. 1,  $D$  is the total laser path length in the instrument. In Eq. (1), the phase difference,  $\phi$ , between the microphone and photodiode signals is assumed to be zero. For typical aerosols in the atmosphere, and nitrogen dioxide at 532 nm, the relaxation time for heat transfer is much faster than the acoustic period at  $f_r \approx 500$  Hz, so  $\phi \approx 0$  when the microphone signal is being produced by light absorption and not ambient noise. In practice, Eq. (1) can be multiplied by  $\cos(\phi)$  to select the in-phase component so that both positive and negative values of  $B_{abs}^{(0)}$  can be obtained, and the light absorption can average to zero as it should when only acoustic noise is present (clean air). Equation (1) is adequate for most ambient sampling conditions, though modifications must be applied when the laser power is strongly attenuated in the resonator. Photoacoustic sound generation is greatest near the pressure antinode in the center of the resonator in Fig. 1, so if the laser beam is strongly attenuated in the resonator, the laser power measured at the photodetector will be less than it actually is near the center. Theory will be developed for the case of strong attenuation in the resonator to set-up the use of high concentrations of light absorbing gas in the resonator for calibration purposes.

The laser beam power absorbed by gas or aerosol in the resonator between distances  $x$  and  $x + dx$ , is a source of time and space varying heat per unit area,  $dH/dA dt$  given by

$$\frac{dH(x,t)}{dA dt} = I(t) \exp[B_{abs}(L+h)] \exp(-B_{abs}x) B_{abs} dx, \quad (2)$$

where  $I(t)$  is the time varying laser beam irradiance measured at the photodetector,  $I(t) \exp\{B_{abs}(L+h)\} \exp(-B_{abs}x)$  is the incident irradiance on the element  $dx$ , and  $B_{abs}$  is the sought-

after light absorption coefficient in dimensions of reciprocal distance. The factor  $\exp\{B_{abs}(L+h)\}$  is used because the laser power measurement is made at ‘pd1’ in Fig. 1, after the beam has potentially been attenuated in the resonator by light absorption. An implicit assumption is that power is removed from the laser beam only by the process of absorption; scattering is assumed negligible.

The acoustic pressure obtained from the time varying heat source in Eq. (2) can be obtained from the resulting wave equation for pressure. To obtain the wave equation, Eq. (2) is related to the thermodynamic properties of the gas, and by combining this with the usual acoustic approximations for gas continuity and the force equation, the wave equation for acoustic pressure is given by

$$\frac{d^2P}{dx^2} - \frac{1}{c^2} \frac{\partial^2 P}{\partial t^2} = -\frac{(\gamma-1)}{c^2} B_{abs} \exp[B_{abs}(L+h)] \exp(-B_{abs}x) \frac{\partial I}{\partial t}, \quad (3)$$

where  $c$  is the speed of sound in the gas. Keep in mind that the irradiance in Eq. (3) is given at the photodetector, and that the irradiance in the resonator drops off exponentially due to absorption in the resonator. Common derivations of the wave equation do not incorporate the exponential decay of laser irradiance explicitly, but assume that this decay is negligible over the resonator length.<sup>15</sup> However, as strong absorption can occur in special cases, such as during calibration with large amounts of absorbing gas or during diesel exhaust analysis, this modification of the wave equation is necessary. Dissipative processes involving gas viscosity and thermal conductivity are not explicitly included in Eq. (3), but are introduced into the normal mode solution now developed.

A general modal solution for photoacoustic signal generation involves expansion of the acoustic pressure in modes of the resonator, determination of the eigen frequencies, mode normalization, and determination of the mode coupling coefficients by computation of the

overlap integral of the light-absorption sound-source determined by the particular arrangement of the laser beam in the resonator.<sup>15</sup> For the special case of the mode and resonator in Fig. 1, the acoustic pressure is given by

$$P(x, f) = \sqrt{2} \sin\left(\frac{\pi x}{L}\right) A(f). \quad (4)$$

The mode coupling coefficient  $A(f)$  is given by

$$A(f) = \frac{-if}{2\pi f_r^2} (\gamma - 1) \frac{1}{2LA_{res}} \frac{\int_0^L \sqrt{2} \sin(\pi x / L) B_{abs} \exp[B_{abs}(L + h)] \exp(-B_{abs}x) dx \int I(f) dA}{1 - \left(\frac{f}{f_r}\right)^2 - i \frac{f}{f_r Q}}, \quad (5)$$

where  $Q$  is introduced as the quality factor to represent dissipation of the acoustic wave due to energy loss in the viscous and thermal boundary layers near the resonator walls, and  $f$  is the acoustic frequency. Note that  $\int I(f) dA = P_L(f)$  is just the Fourier component at frequency  $f$  of the time varying laser power, and that the resonator open volume is  $2LA_{res}$  where  $A_{res}$  is the resonator cross sectional area. The superscript is dropped on the absorption coefficient, as it now represents the actual value of this quantity.

Solution of the integral in Eq. (5) leads to an analytical form for  $A(f)$  as

$$A(f) = \frac{\frac{-if}{\sqrt{2}\pi^2 f_r^2 A_{res}} (\gamma - 1) B_{abs} P_L(f)}{1 - \left(\frac{f}{f_r}\right)^2 - i \frac{f}{f_r Q}} \left\{ \frac{\exp[B_{abs}(L + h)] [1 + \exp(-B_{abs}L)]}{2 \left[ 1 + \left(\frac{B_{abs}L}{\pi}\right)^2 \right]} \right\}. \quad (6)$$

The term in curly brackets is not present in common solutions of the photoacoustic equation, and it has some illuminating behavior for certain limits. When the absorption optical depth is very small, ( $B_{abs}L \ll 1$ ), as is typical in most ambient applications of photoacoustic methods, then the term in curly brackets tends to unity. However, for very large absorption optical depth, it tends

to zero, which has the simple physical interpretation that if all the laser power is absorbed a very short distance into the resonator, no sound can be generated.

For ( $B_{abs}L < 0.2$ ), the term in curly brackets can be approximated with a percentage error less than 0.6% as

$$\left\{ \frac{\exp[B_{abs}(L+h)][1 + \exp(-B_{abs}L)]}{2 \left[ 1 + \left( \frac{B_{abs}L}{\pi} \right)^2 \right]} \right\} \approx \left\{ 1 + \frac{B_{abs}D}{2} \right\}, \quad (7)$$

where  $B_{abs}D$  is the absorption optical depth for the laser path in the instrument (see Fig. 1). For larger absorption optical depths, more terms can be taken in the expansion.

At resonance, the acoustic pressure at the microphone location  $x = -L/2$  is

$$P_{mic}(f_r) \equiv -P(x = -L/2, f_r) = \frac{Q}{\pi^2 f_r A_{res}} (\gamma - 1) P_L(f_r) B_{abs} \left\{ 1 + \frac{B_{abs}D}{2} \right\}, \quad (8)$$

where the approximate form, Eq. (7) of the term in curly brackets from Eq. (6), has been used, along with the pressure modal profile in Eq. (4). The minus sign in Eq. (8) is just the  $\pi$  phase difference between the laser power Fourier component and the microphone pressure, (i.e. the phase difference between the pressure antinode at the resonator center and at the microphone locations in Fig. 1). The phase of the microphone measured signal is shifted by  $\pi$  in practical measurements. To the same level of approximation of the term in curly brackets in Eq. (8), the desired absorption coefficient can be obtained from

$$B_{abs}^{(1)} = B_{abs}^{(0)} \left\{ 1 - B_{abs}^{(0)} \frac{D}{2} \right\}, \quad (9)$$

where  $B_{abs}^{(0)}$  is given in Eq. (1), and superscript (1) now refers to the absorption coefficient with a first order correction for laser beam attenuation in the resonator. The physical interpretation of Eq. (9) is that since the laser beam power is measured at the detector, it appears to be less than

the value near the center of the resonator where photoacoustic sound generation occurs, so Eq. (1) would overpredict the absorption coefficient. (For ambient sampling applications,  $B_{abs} < 10^{-5} \text{ m}^{-1}$  is typical, so the term in curly brackets can safely be set to unity, and Eq. (1) can be used to obtain the absorption coefficient.) Keep in mind that use of Eq. (9) implies that the absorption optical depth is  $B_{abs}L < 0.2$ .

In actual measurements, it is convenient to use complex quantities for the microphone pressure and laser power in Eq. (1), to obtain the complex ratio, and to use the in-phase component. It is also convenient to measure the ratio with the same A/D channel so that any changes or drifts in the A/D calibration occur on both measurements, and thus are cancelled.

The gas transmission coefficient,  $T$ , is given by

$$T = \frac{P_L}{P_L^{(o)}} = \frac{\int \frac{dP_L^{(o)}(\lambda)}{d\lambda} \exp(-B_{abs}(\lambda)D) d\lambda}{P_L^{(o)}} , \quad (10)$$

where  $\lambda$  is the optical wavelength,  $dP_L^{(o)}(\lambda)/d\lambda$  is the laser power spectral density,  $P_L^{(o)} = \int (dP_L^{(o)}(\lambda)/d\lambda) d\lambda$  is the laser power measured at the detector before the resonator is filled with  $\text{NO}_2$ , and the numerator is the integrated monochromatic attenuation. The approximation that Rayleigh scattering can be ignored relative to absorption has been made, though of course, it could be calculated and added to  $B_{abs}(\lambda)$  to form the true extinction coefficient if desired. A first approximate form of Eq. (10) is obtained for a small argument (for all  $\lambda$ ) in the exponential term of Eq. (10),

$$T \approx \frac{\int \frac{dP_L^{(o)}(\lambda)}{d\lambda} \{1 - B_{abs}(\lambda)D\} d\lambda}{P_L^{(o)}} \equiv 1 - B_{abs}D . \quad (11)$$

Another common approximation of Eq. (10) is Beer's law,

$$T \approx \exp(-B_{abs}D) , \quad (12)$$

where the assumption is that either the light source is highly monochromatic, or that the variation of the absorption coefficient is negligible throughout the wavelength range of appreciable source power spectral density. The absorption coefficient can be obtained from the first approximate form as ,

$$B_{abs} \approx \frac{1-T}{D}, \quad (1-T \ll 1) . \quad (13)$$

And it can be obtained from Beer's law as

$$B_{abs} \approx \frac{-\ln(T)}{D}, \quad (\text{approximately monochromatic}). \quad (14)$$

It can be seen that Eq. (13) is obtained from Eq. (14) when  $(1-T) \ll 1$ . Assuming for the moment that the Beer's law approximation of Eq. (14) is valid, then the error one obtains from use of Eq. (13) when  $T > 0.925$  is less than 3.8% (this number is appropriate for the conditions reported here). The approximate form, Eq. (14), is used to obtain an estimate for the absorption coefficient from the transmission measurements, both because the laser is approximately monochromatic, and because the measured transmission range makes the use of the approximation of Eq. (13) reasonably valid. In other words, the Beer's law approximation used to obtain Eq. (14) is not so strongly restrictive to monochromatic radiation when  $1 - T \ll 1$ , though it is emphasized that the discussion below Eq. (12) should be kept in mind when using this approximation. The use of Eq. (9) to obtain a first order correction for the absorption coefficient obtained by the photoacoustic method (for the case of strong attenuation) implies the same approximation as the use of Beer's law in Eq.(14).

Transmission is measured by splitting the laser beam at the entrance to instrument (beam splitter shown in Fig. 1), and using a second photodetector to serve as a laser power reference (pd2 in Fig. 1). The rest of the beam passes through the instrument as normal. Then by

performing a referenced-laser power measurement, the transmission coefficient is obtained as the ratio of during-sample to before-sample powers. This method avoids determination of instrument window transmission coefficients.

The absorption coefficient can be obtained from a photoacoustic measurement as indicated by Eqs. (1) and (9), or from a transmission measurement by using Eq. (14). The comparison of these methods, and published absorption coefficients for NO<sub>2</sub> will be considered in the next section.

### **3. Measurement of absorption coefficient of NO<sub>2</sub>, and evaluation of the photoacoustic equation.**

The photoacoustic instrument used is similar to an earlier version,<sup>5</sup> and the main differences will be discussed here. The new instrument is constructed of stainless steel, instead of copper in the previous instrument, but both have the geometry shown in Fig. 1. The nominal acoustic resonance frequency is  $f_r=494$  Hz, quality factor is  $Q=49$ , cross sectional area is  $A_{res}=2.34$  cm<sup>2</sup>, and the laser path length in the instrument as shown in Fig. 1 is  $D=48.9$  cm. The diameter of the tubing in the resonator is less than the previous instrument, which lowers the quality factor some, but overall increases the sound amplitude produced by light absorption. This smaller diameter better adapts to the microphone used to measure sound, and to the piezoelectric disk used for acoustic calibration. The modest  $Q$  keeps the acoustic bandwidth sufficiently wide that slight temperature changes, and associated resonance frequency changes, do not comprise the light absorption measurement between acoustic calibrations. Yet, the  $Q$  is high enough that holes can still be placed in the resonator at pressure nodes, and ambient acoustic noise does not couple well through these holes to the mode being driven.<sup>16</sup>

Figure 2 shows the schematic arrangement used to pull  $\text{NO}_2$  through the photoacoustic instrument for calibration purposes. Some care must be exercised to ensure that the photoacoustic instrument is not rapidly pressurized so that the microphone membrane is forced against the back plate and shorted. To help prevent pressurization problems, a pressure-equalization tube is used from the sample outlet line on the resonator to the back face of the microphone so that no DC pressure exists across the microphone membrane. The equalization tube is connected directly to the vent port on the microphone. This port is designed to have a very high flow resistivity so that sound does not effectively travel through it. A desiccant is placed in the equalization tube to keep the back face of the microphone membrane dry. It is also critical to use the equalization tube when the sample inlet to the instrument is below ambient pressure; otherwise, the microphone membrane is drawn away from the back plate, and being essentially a parallel plate capacitor, the microphone calibration becomes uncertain.

Before the valve in the gas cylinder in Fig. 2 is open, the pump pulls air from the exhaust, through the air-rotometer, and through the instrument. The ball in the air rotometer is elevated in this situation. When the gas cylinder valve is opened, the ball in the  $\text{NO}_2$ -rotometer is now elevated, and the ball in the air-rotometer returns to its rest position. This indicates that  $\text{NO}_2$  in  $\text{N}_2$  is being pulled through the instrument. The use of two rotometers ensures a gas path of either air or calibration gas through the instrument at all times. Ambient pressure, temperature, and relative humidity sensors are placed on the outlet of the photoacoustic instrument. Since the ambient sound speed is proportional to the square root of the average gas molecular weight, the acoustic resonance frequency increases from about 494 Hz to about 500 Hz because of the  $\text{N}_2$  gas. Effects of dispersion due gas composition changes, and associated viscosity and thermal conductivity changes, are not as dramatic as the molecular weight influence on resonance

frequency. In any case, the ratio of constant pressure and constant volume heat capacities in Eq. (1) remains nominally the same as for air, and the acoustic calibration with the piezoelectric transducer is used to determine  $f_r$  and  $Q$ .

The average absorption coefficient measured with the photoacoustic method is shown in Fig. 3 along with high resolution measured absorption spectra of NO<sub>2</sub>.<sup>17</sup> The wavelength for the laser-diode-pumped, solid-state, frequency-doubled laser<sup>18</sup> is nominally 532.0 nm, though the precise spectrum will depend on its longitudinal mode structure. In addition, the stated accuracy of the NO<sub>2</sub> concentration is  $\pm 5\%$  by the manufacturer. In principle, the average photoacoustic absorption coefficient should be compared with the spectral curve shown in bold, at a wavelength of 532.00 nm; however, it is likely that the comparison could be made to any value bracketed by the spectral curves computed from the uncertainty in NO<sub>2</sub> concentration. From the measured high resolution spectrum, and the uncertainty in gas concentration, the expected photoacoustic absorption coefficient could lie with the range of 133,000 Mm<sup>-1</sup> to 174,000 Mm<sup>-1</sup>. The average value, 156,000 Mm<sup>-1</sup>  $\pm$  1,000 Mm<sup>-1</sup>, where the uncertainty was derived from the standard deviation, does lie in this range, though without much more detailed measurement of laser spectrum, and improved gas concentration measurement, more definitive statements about the accuracy of the photoacoustic measurement can not be made. Before the discussion turns to use of extinction measurements to improve upon the statement of the accuracy, some discussion of the factors influencing photoacoustic accuracy and precision will now be considered.

Refer to Eq. (1) for the parameters that must be measured in the photoacoustic method. The microphone pressure is measured using a calibrated microphone and phase-sensitive detection so that the signal to noise ratio of this measurement is dependent on the square root of the averaging time.<sup>14</sup> Microphone calibration is accomplished with a piston-driver device

manufactured for this purpose, and is accurate to within 2%. Calibration drift has been negligible in the authors' experience. The laser power measurement is performed in the same manner as the microphone measurement (phase-sensitive detection by use of a fast detector; secondary calibration of the detector with a laser power meter). The cross sectional area of the resonator is measured once. The ratio of specific heats for air (and  $N_2$ ) is taken to be 1.4. The acoustic calibration of the resonator is accomplished with the piezoelectric disk and microphone using a high-spectral-resolution scan below, at, and beyond the resonance frequency, and a curve fit to this measurement with adjustable parameter of resonance frequency, quality factor, and peak pressure. As a result, the accuracy and precision of the resonance frequency and quality factor are better than 0.2% and 1%, respectively. A programmable preamplifier is used to condition the microphone signal before the analog to digital converter board on the computer (A/D). The same A/D is used for both microphone and photodetector signals, so gain error here will be compensated, as these quantities enter Eq. (1) as a ratio. The signal to noise ratio of the microphone measurement is dependent on just how much light absorption is present, and on the length of the integration time. The agreement of measured light absorption by  $NO_2$  using the photoacoustic method, and the independently-measured spectra as shown in Fig. 3 is a reassurance that the photoacoustic equations (Eqs. (1) and (9)) are valid.

The comparison of light absorption and extinction measurements (Eqs (9) and (14)) is shown in Fig. 4. The extinction method is discussed in the paragraph following the development of Eq. (14). The main uncertainty in the extinction measurement is the determination of the instrument path length,  $D$ . Note that the fluctuation of the extinction measurement is greater than that of the absorption measurement. Fluctuations of the laser power between measurements with the two photodiodes in Fig. 1 gives rise to the extinction fluctuations. These fluctuations

limit the accuracy of the extinction measurement (but negligibly influence the absorption measurement). The measurements of extinction and absorption are in close agreement. The range of uncertainty in the extinction measurement, indicated by the bracketing curves in Fig. 4, is considerably less than the range in Fig. 3. Using the extinction measurement as a direct evaluation of the calibration of the absorption measurement is relatively simple, and it does not require accurate determination of the laser and gas spectra, or the gas concentration.

However, be cautioned that the extinction measurement will not always be equal to the photoacoustic absorption measurement at all wavelengths. A nice demonstration of this limitation is seen in the combined extinction and photoacoustic spectra of  $\text{NO}_2$  ranging from the UV into the visible.<sup>8</sup> For wavelengths shorter than 397.9 nm,  $\text{NO}_2$  photodissociates into  $\text{O} + \text{NO}$ . In other words, not all of the absorbed photon energy is converted to heat in the surrounding gas; some is used in breaking up the molecule. Judicious choice of absorbing gas should compensate this problem if the method needs to be expanded to other wavelengths.

#### **4. Measurement of absorption and extinction coefficients of kerosene-flame soot at 532 nm and 1047 nm.**

Two photoacoustic instruments were used to simultaneously measure light absorption and extinction at two wavelengths, 532 nm and 1047 nm. The instrument equipped with a 1047 nm laser has been used to measure the black carbon content of vehicle exhaust in real time. This laser can be electronically modulated to achieve phase sensitive detection and locking to the resonance acoustic frequency. While the instrument equipped with a 532 nm laser can be calibrated using  $\text{NO}_2$ , the other one can not because light absorption by this gas is very weak at 1047 nm. However, it is argued in this section that the instrument equipped with a 1047 nm laser

can provide accurate measurements of aerosol light absorption through the use of the photoacoustic equations, Eq. (1) and Eq. (9).

Figure 5 shows the schematic arrangement used to measure optical properties of kerosene-flame soot. A standard kerosene lamp was lit, and the wick was placed higher than normal so that a copious amount of soot was produced. The soot was mixed, by way of a valve, with filtered dilution air, and conveyed in the copper-tubing sample line to the photoacoustic instruments. The inlet was placed high enough above the flame to prevent direct heating, and to allow the soot-laden air to cool before entering it. An adequate range of relatively steady aerosol concentrations was obtained. The two photoacoustic instruments were equipped with lasers operating at 532 nm and 1047 nm, respectively, and simultaneously measured light absorption and extinction at these wavelengths. The instrument equipped with a 1047 nm laser was described previously,<sup>5</sup> though it was operated at the next useful higher frequency ( $\approx 1500$  Hz) instead of the usual 500 Hz frequency to reduce the effects of ambient acoustic noise on the instrument. The theoretical photoacoustic equation for this mode of operation is obtained by multiplying Eq. (1) by a factor of three (three half acoustic wavelengths are pumped by the laser beam in Fig. 1 when this mode is used instead of just one.) The instrument equipped with a 532 nm laser operated at 1500 Hz, and is based on an acoustic resonator 1/3 the size of the other one so that the mode symmetry is as outlined in Fig. 1. To accomplish this smaller design, the two portions of the resonator shown in Fig. 1 that are on each end (and are bent at a 45 deg. angle relative to the horizontal) were actually made at a 90 deg. angle. The larger angle simplified construction, but did not hinder performance. This instrument was calibrated using the NO<sub>2</sub> method described in the previous section.

A particle filter was placed over the inlet in Fig. 5 to evaluate the response of the photoacoustic instruments to the gases generated by the kerosene flame. The inlet through the filtered-air path in Fig. 5 was closed for this measurement. The light absorption results are shown in Fig. 6. The 532 nm light absorption is due to NO<sub>2</sub> generated by the flame, as was verified by placing a NO<sub>2</sub> denuder<sup>19</sup> after the particle filter in measurements obtained earlier. The denuded sample air produced only background levels of light absorption, similar to that obtained with the 1047 nm laser instrument (Fig. 6). The NO<sub>2</sub> concentration in the exhaust was estimated to be 330 ppb based on the calibration performed earlier by the method described in the previous section. The particle-free measurements provided some insight into the amount of NO<sub>2</sub> generated by a kerosene flame, but also show that the light absorption due to exhaust gases is very small in comparison to the values generated by aerosol laden air, as discussed next.

Measurements of optical properties of kerosene-flame soot are shown in Fig. 7 at the two laser wavelengths as a function of time, and are summarized as average values in Table 1. Theory for light absorption in the dipole limit indicates that  $B_{abs}$  should vary inversely with wavelength when the complex refractive index remains constant, and that the single scattering albedo is a complicated function of particle geometry, refractive index, and particle size.<sup>20</sup> The theoretical ratio  $B_{abs}(532 \text{ nm})/B_{abs}(1047) \approx 1047/532 = 1.97$  compares favorably with the value 1.95 from measurement. The light absorption axes in Figs. 7a) and 7b) are scaled by a factor of 2 to demonstrate this approximate wavelength scaling. The photoacoustic method can be evaluated at other wavelengths using kerosene soot when coupled with a measurement at 532 nm that has been evaluated using the methods described in the previous section.

The single scattering albedo was computed from  $\omega_o = (B_{ext} - B_{abs})/B_{ext}$ , and values different from zero are shown in Fig. 7 when a quasi steady-state concentration of soot has been obtained

in the instrument. Scattering is reduced at longer wavelengths, so  $B_{ext}$  is closer in value to  $B_{abs}$  in Fig. 7b) than in Fig. 7a). The single scattering albedo is 0.20 and 0.31 at wavelengths of 1047 nm and 532 nm, respectively. For comparison, the burning of various fuels (petrol, diesel, fuel oil, paraffin oil, butane, and wood) and subsequent measurement of the single scattering albedos produces values of (0.28, 0.30, 0.31, 0.26, 0.24, and 0.62), respectively, at a wavelength of 632 nm.<sup>21</sup>

## 5. Discussion.

The analytical description for the calibration of the photoacoustic instrument has been extended to include strong absorption of the laser beam in the instrument (Eqs. (1) and (9)). This case applies to calibration using high concentrations of absorbing gas. The photoacoustic method of obtaining the absorption coefficient agrees well with both a high spectral-resolution spectrum of NO<sub>2</sub>, and simultaneous extinction measurement by NO<sub>2</sub> in the photoacoustic instrument. The extinction calibration is relatively simple, does not require precise knowledge of the absorbing-gas concentration, and avoids the requirement of detailed gas and laser spectra. In summary, the photoacoustic equations (Eqs. (1) and (9)) appear to provide an accurate description of the absorption coefficient as measured with this instrument. The single scattering albedo for kerosene-flame soot was measured at 532 nm and 1047 nm using two photoacoustic instruments as another application of the simultaneous extinction and absorption measurement method. The use of transmission measurements to calibrate a Helmholtz-resonator photoacoustic-instrument has been described,<sup>22</sup> and is an example of the basic methodology described in the current paper as applied to a rather different wavelength range and spectroscopic analysis.

## **Acknowledgements**

Development of the photoacoustic instrument was supported by the National Science Foundation, grant ATM-9871192, the US Department of Energy under cooperative agreement DE-FC02-98EE50563, and the Applied Research Initiative of the State of Nevada. Calibration was supported in part by the National Oceanic and Atmospheric Agency through the Cooperative Institute for Atmospheric Sciences and Terrestrial Applications (CIASTA) for the Big Bend Regional Aerosol and Visibility Observational Study, and by the Strategic Environmental Research and Development Program (SERDP). Insightful conversations with William Stockwell and C. Fred Rogers are acknowledged.

## REFERENCES

- <sup>1</sup>D. G. Fox, W. C. Malm, B. Mitchell, and R. W. Fisher, "Where there's fire there's smoke," in *EM, Air and Waste Management Association* (1999), pp. 15-24.
- <sup>2</sup>H. Horvath, *Atmos. Env.* **27A** (3), 293-317 (1993).
- <sup>3</sup>T. C. Bond, T. L. Anderson, and D. Campbell, *Aer. Sci. Tech.* **30** (6), 582-600 (1999).
- <sup>4</sup>K. M. Adams, L. I. Davis, Jr., S. M. Japar, D. R. Finley, and R. A. Cary, *Atmos. Env.* **24A**, 597-604 (1990).
- <sup>5</sup>W. P. Arnott, H. Moosmüller, C. F. Rogers, T. Jin, and R. Bruch, *Atmos. Env.* **33**, 2845-2852 (1999).
- <sup>6</sup>H. Moosmüller, W. P. Arnott, C. F. Rogers, J. C. Chow, C. A. Frazier, L. E. Sherman, and D. L. Dietrich, *J. Geophys. Res.* **103, D21**, 28149-28157 (1998).
- <sup>7</sup>A. Petzold and R. Niessner, *Appl. Phys.* **B 63**, 191-197 (1996).
- <sup>8</sup>W. R. Harshbarger and M. B. Robin, *Acc. Chem. Res.* **6** (10), 329-334 (1973).
- <sup>9</sup>M. W. Sigrist, in *Chemical analysis series*, edited by Marcus W. Sigrist (John Wiley & Sons, Inc., New York, 1994), Vol. 127, pp. 163-238.
- <sup>10</sup>R. P. Fiegel, P. B. Hays, and W. M. Wright, *Appl. Opt.* **28**, 1401-1408 (1989).
- <sup>11</sup>D. M. Roessler, *Appl. Opt.* **23**, 1148-1155 (1984).
- <sup>12</sup>K. M. Adams, *Appl. Opt.* **27**, 4052-4056 (1988).
- <sup>13</sup>A. Petzold and R. Niessner, *Appl. Phys. Lett.* **66** (10), 1285-1287 (1995).
- <sup>14</sup>W. P. Arnott, H. Moosmüller, R. E. Abbott, and M. D. Ossofsky, *Rev. Sci. Ins.* **66** (10), 4827-4833 (1995).
- <sup>15</sup>A. Rosencwaig, *Photoacoustics and photoacoustic spectroscopy* (Wiley, New York, NY, 1980).

<sup>16</sup>Images of the instrument can be viewed at <http://www.dri.edu/Projects/replica/photoacoustic/>.

<sup>17</sup>J. W. Harder, J. W. Brault, P. V. Johnston, and G. H. Mount, *J. Geophys. Res.* **102** (D3), 3861-3879 (1997).

<sup>18</sup>Crystalaser, manufacturer

<sup>19</sup>K. M. Adams, S. M. Japar, and W. R. Pierson, *Atmos. Env.* **20** (6), 1211-1215 (1986).

<sup>20</sup>K. A. Fuller, W. C. Malm, and S. M. Kreidenweis, *J. Geophys. Res.* **104** (D13), 15 (1999).

<sup>21</sup>I. Colbeck, B. Atkinson, and Y. Johar, *Journal of Aerosol Science* **28**, 715-723 (1997).

<sup>22</sup>R. Kästle and M. W. Sigrist, *Appl. Phys. B* **63**, 389-397 (1996).

.

## Tables

**Table 1.** Measured aerosol optical properties for kerosene-flame soot. Uncertainties in single scattering albedo were computed from the standard deviation of 16 measurements.

	<b>Average values at 532 nm</b>	<b>Average values at 1047 nm</b>
<b>Extinction (<math>Mm^{-1}</math>)</b>	241,000	107,000
<b>Absorption (<math>Mm^{-1}</math>)</b>	166,000	85,400
<b>Single Scattering Albedo</b>	$0.31 \pm 0.01$	$0.20 \pm 0.01$

## Figure Captions

**Figure 1.** Schematic of a plane wave resonator used for photoacoustic measurements. The locations of pressure nodes (p.n.) and pressure antinodes (p.a.) are shown. The power modulated laser beam pumps the acoustic wave via light absorption as a periodic heat source in the center region between pressure nodes. The length of the laser-pumping path in the resonator is denoted as  $L$ . The definition of a position coordinate  $x$  is shown. The acoustic resonator is highlighted in bold lines. 'pd' refers to photodetector, 'bs' to beam splitter.

**Figure 2.** Schematic of arrangement used to deliver nitrogen dioxide through the photoacoustic instrument. The air-rotometer path allows air to be pulled through the instrument when the  $\text{NO}_2\text{-N}_2$  valve is off.

**Figure 3.** High resolution measured  $\text{NO}_2$  spectra at the nominal concentration of 509 ppm (bold line) as computed for the pressure and temperature stated in the graph. The thin lines indicate the high-resolution spectra calculated for the range of concentration uncertainty indicated in the graph. The average measured photoacoustic light absorption coefficient for  $\text{NO}_2$  (dashed line) was measured only at the laser wavelength. The nominal laser wavelength is 532.0 nm, though the laser spectrum will depend on the longitudinal modes operating at any time.

**Figure 4.** Measurements of the absorption coefficient of  $\text{NO}_2$  using the photoacoustic method (dashed line) and the extinction method (bold line), showing good agreement between these methods. The thin lines are bounds for the estimated uncertainty of the extinction measurement. Note the compressed scale of this figure compared to the previous figure, indicating a more definitive evaluation of the photoacoustic method.

**Figure 5.** Schematic arrangement for kerosene-flame soot generation and measurement with two photoacoustic instruments. The wick in the kerosene lamp is raised high enough to produce copious amounts of soot, and the valve is used to control the dilution with filtered air.

**Figure 6.** Observed light absorption when a particle filter was put over the kerosene flame inlet in figure 5. The low  $B_{abs}$  at 1047 nm indicates that the particle filter was operating correctly. The combustion-generated  $\text{NO}_2$  passed by the filter is responsible for the  $B_{abs}$  at 532 nm.

**Figure 7.** Measured extinction, absorption, and calculated single scattering albedo for kerosene flame soot and a wavelength of A) 532 nm, and B) 1047 nm. Note especially that the  $B_{abs}$  at 1047 nm is approximately half that of the 532 nm wavelength value.

FIGURES

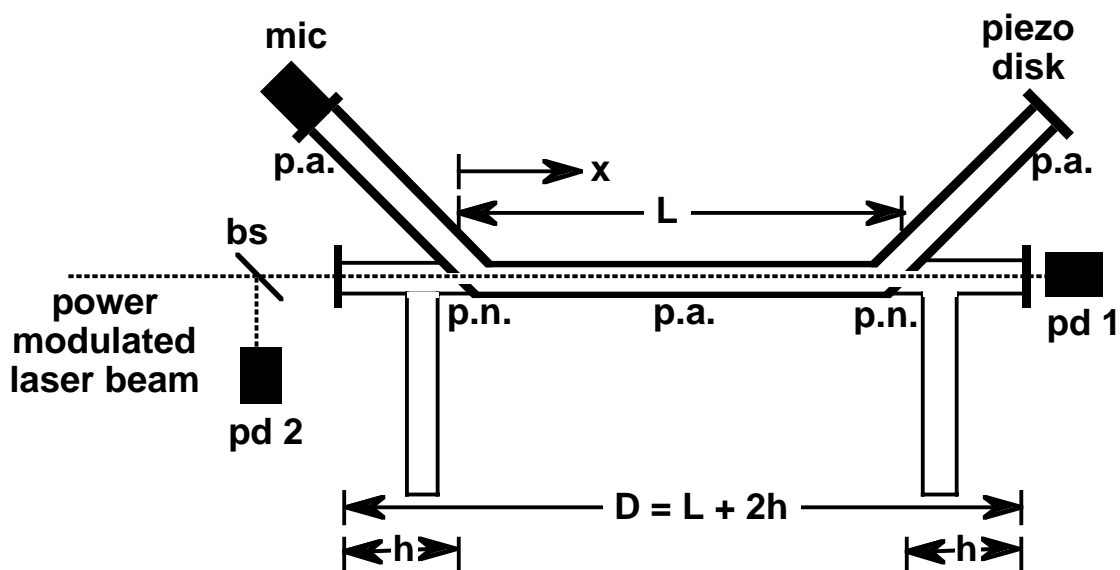


**Figure 1.** Schematic of a plane wave resonator used for photoacoustic measurements. The locations of pressure nodes (p.n.) and pressure antinodes (p.a.) are shown. The power modulated laser beam pumps the acoustic wave via light absorption as a periodic heat source in the center region between pressure nodes. The length of the laser-pumping path in the resonator is denoted as  $L$ . The definition of a position coordinate  $x$  is shown. The acoustic resonator is highlighted in bold lines. ‘pd’ refers to photodetector, ‘bs’ to beam splitter.

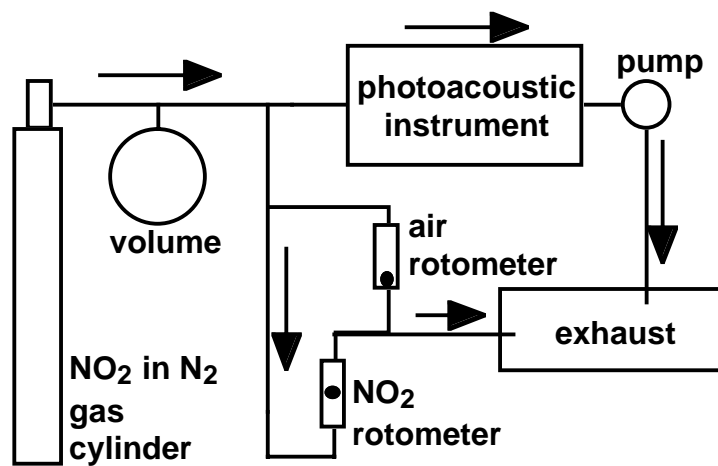


**Figure 2.** Schematic of arrangement used to deliver nitrogen dioxide through the photoacoustic instrument.

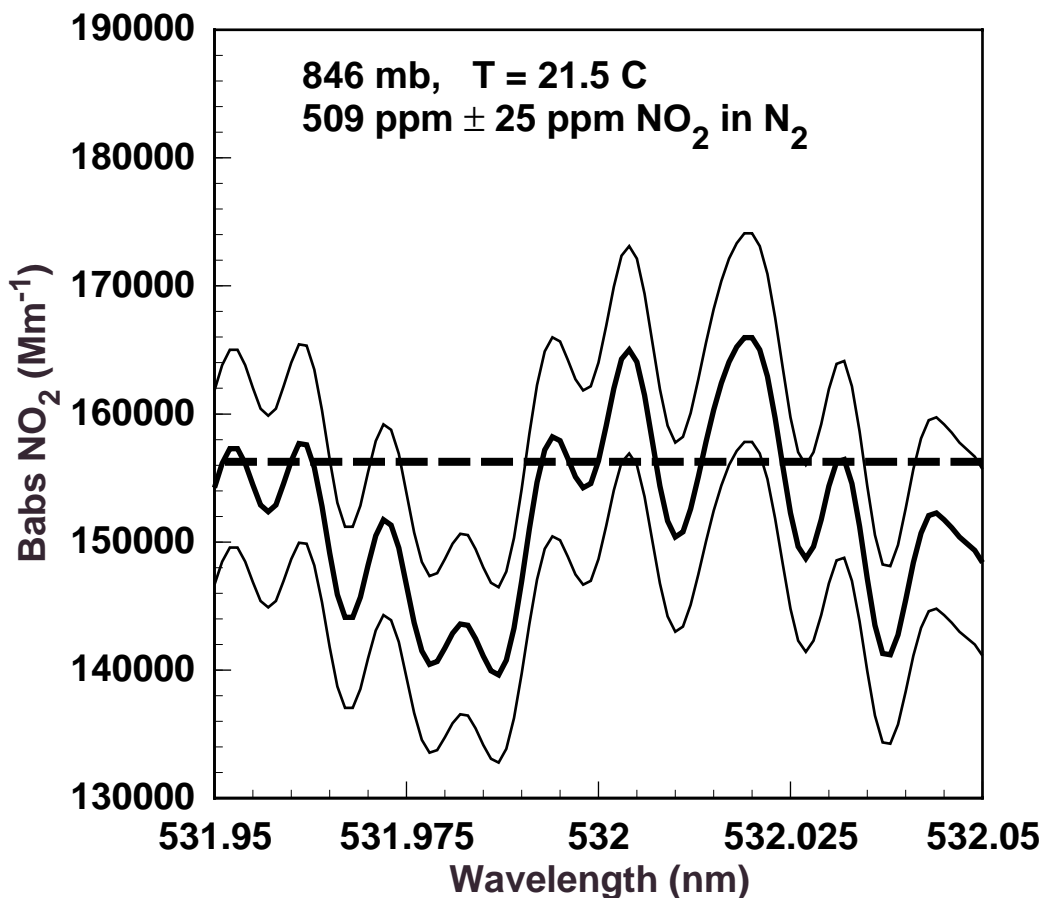


**Figure 3.** High resolution measured NO<sub>2</sub> spectra at the nominal concentration of 509 ppm (bold line) as computed for the pressure and temperature stated in the graph. The thin lines indicate the high-resolution spectra calculated for the range of concentration uncertainty indicated in the graph. The average measured photoacoustic light absorption coefficient for NO<sub>2</sub> (dashed line) was measured only at the laser wavelength. The nominal laser wavelength is 532.0 nm, though the laser spectrum will depend on the longitudinal modes operating at any time.

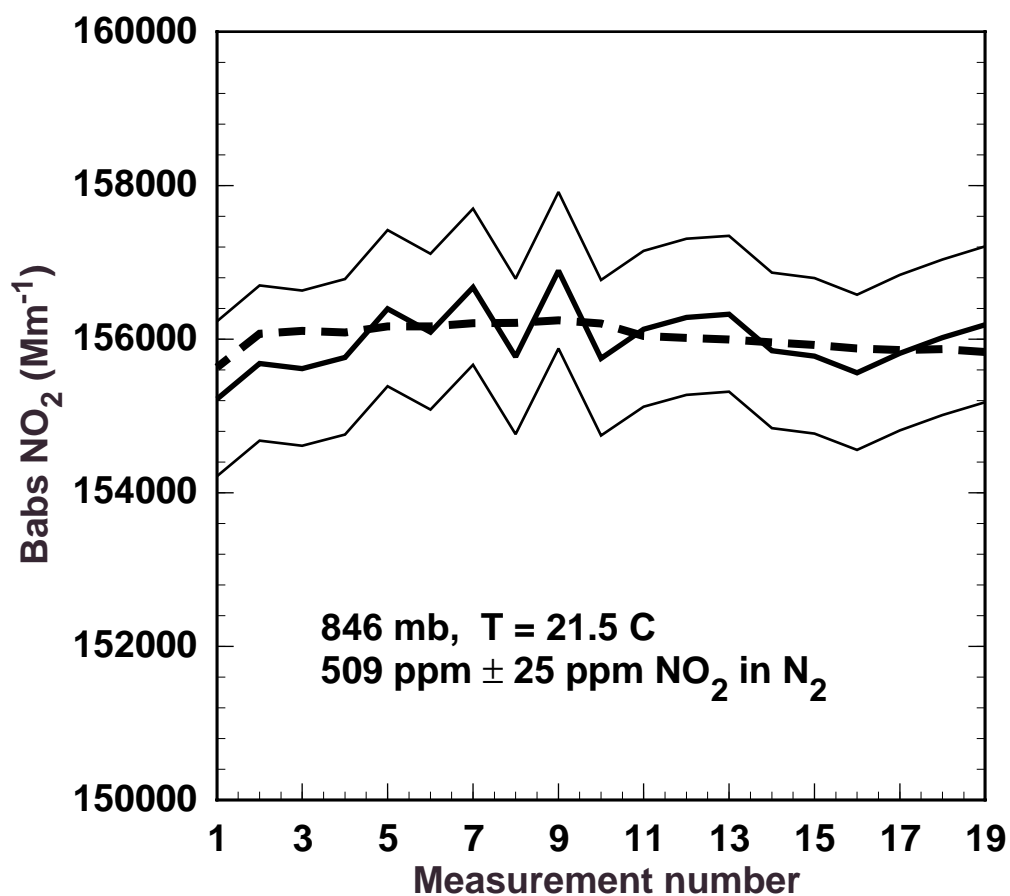


**Figure 4.** Measurements of the absorption coefficient of NO<sub>2</sub> using the photoacoustic method (dashed line) and the extinction method (bold line), showing good agreement between these methods. The thin lines are bounds for the estimated uncertainty of the extinction measurement. Note the compressed scale of this figure compared to the previous figure, indicating a more definitive evaluation of the photoacoustic method.

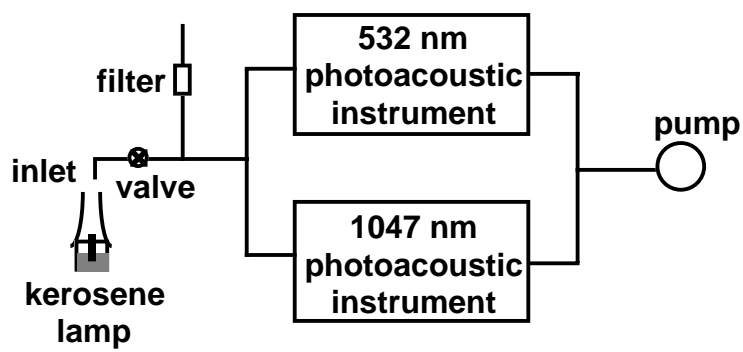


**Figure 5.** Schematic arrangement for kerosene-flame soot generation and measurement with two photoacoustic instruments. The wick in the kerosene lamp is raised high enough to produce copious amounts of soot, and the valve is used to control the dilution with filtered air.

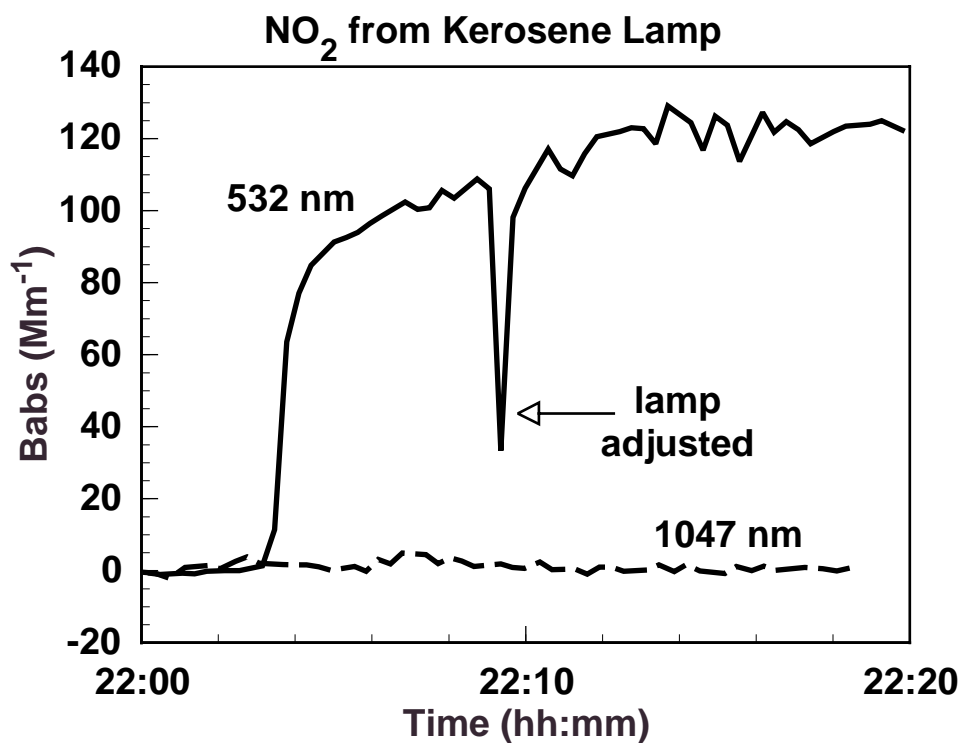


**Figure 6.** Observed light absorption when a particle filter was put over the kerosene flame inlet in figure 5. The low  $B_{abs}$  at 1047 nm indicates that the particle filter was operating correctly. The combustion-generated NO<sub>2</sub> passed by the filter is responsible for the  $B_{abs}$  at 532 nm.

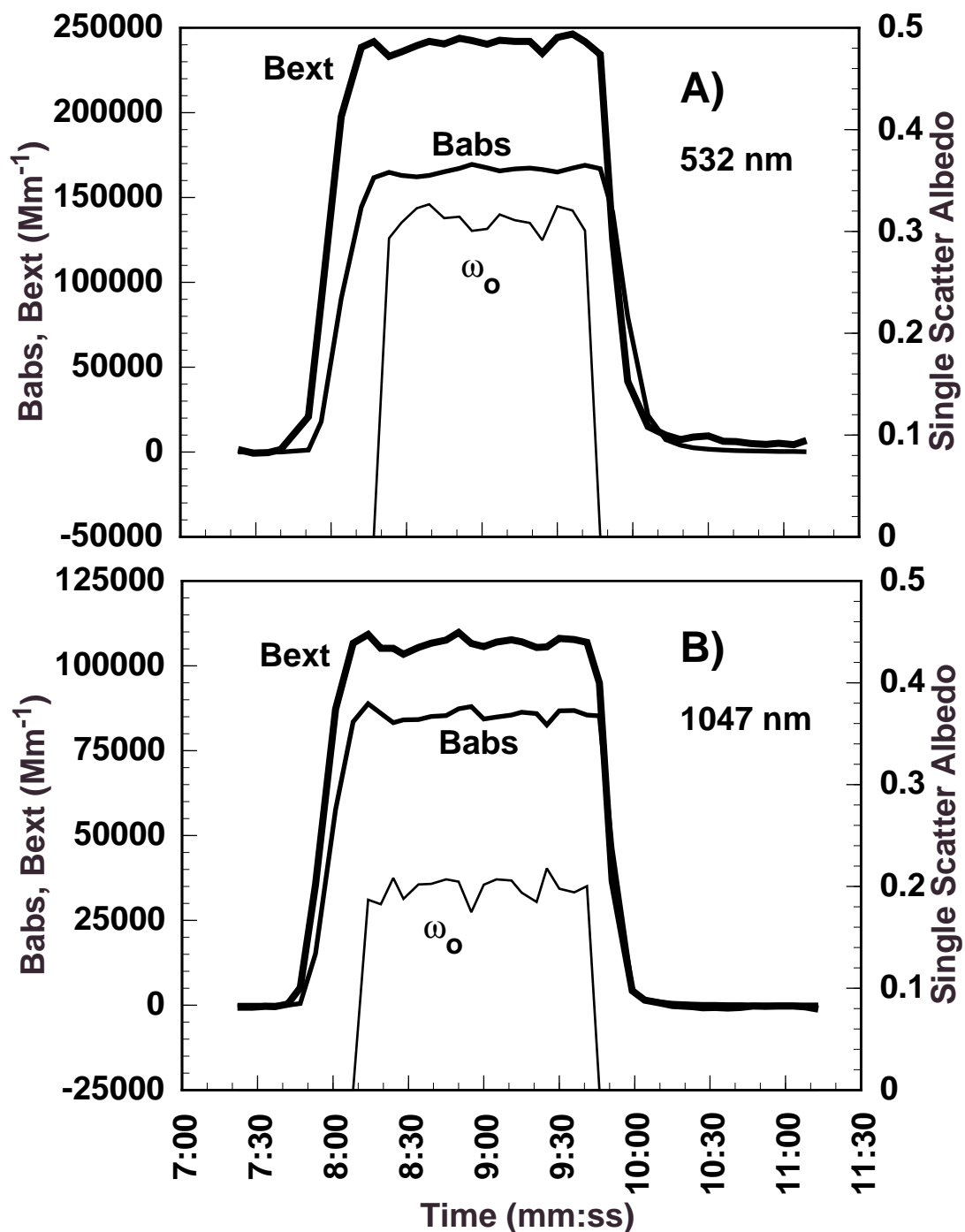


**Figure 7.** Measured extinction, absorption, and calculated single scattering albedo for kerosene flame soot and a wavelength of A) 532 nm, and B) 1047 nm. Note especially that the  $B_{abs}$  at 1047 nm is approximately half that of the 532 nm wavelength value.